

On Deep Learning Solutions for Joint Transmitter and Noncoherent Receiver Design in MU-MIMO Systems

Songyan Xue, Yi Ma, Na Yi, and Rahim Tafazolli

Institute for Communication Systems (ICS), University of Surrey, Guildford, England, GU2 7XH

E-mail: (songyan.xue, y.ma, n.yi, r.tafazolli@surrey.ac.uk)

Abstract—This paper aims to handle the joint transmitter and noncoherent receiver design for multiuser multiple-input multiple-output (MU-MIMO) systems through deep learning. Given the deep neural network (DNN) based noncoherent receiver, the novelty of this work mainly lies in the multiuser waveform design at the transmitter side. According to the signal format, the proposed deep learning solutions can be divided into two groups. One group is called pilot-aided waveform, where the information-bearing symbols are time-multiplexed with the pilot symbols. The other is called learning-based waveform, where the multiuser waveform is partially or even completely designed by deep learning algorithms. Specifically, if the information-bearing symbols are directly embedded in the waveform, it is called systematic waveform. Otherwise, it is called non-systematic waveform, where no artificial design is involved. Simulation results show that the pilot-aided waveform design outperforms the conventional zero forcing receiver with least squares (LS) channel estimation on small-size MU-MIMO systems. By exploiting the time-domain degrees of freedom (DoF), the learning-based waveform design further improves the detection performance by at least 5 dB at high signal-to-noise ratio (SNR) range. Moreover, it is found that the traditional weight initialization method might cause a training imbalance among different users in the learning-based waveform design. To tackle this issue, a novel weight initialization method is proposed which provides a balanced convergence performance with no complexity penalty.

I. INTRODUCTION

Multiuser multiple-input multiple-output (MU-MIMO) systems have been extensively studied in the past few decades for their advantages on increasing system capacity, enhancing spectrum efficiency and improving link reliability [1]. A fundamental problem for MU-MIMO system is to estimate the transmitted signal relying on the knowledge of the received signal and the channel. To elaborate a little further, if the instantaneous channel state information (CSI) is available at the receiver, the detection of the transmitted signal relies on coherent detection; and there exists a wide range of solutions in the traditional communication domain [2]. Things become difficult when the CSI is avoided, i.e., MU-MIMO signal detection belongs to the family of noncoherent detection [3]. In this case, one of the most commonly used methods is called differential encoding, which imposes correlation among the transmitted symbols [4]. And the receiver needs to use sequence-level differential detection which leads to a higher computational complexity and a degraded power efficiency compares with the symbol-level coherent detection algorithms. Therefore, noncoherent detection is normally considered to suffer an inherent performance loss unless the block size is sufficiently large [1].

Recent advances towards noncoherent MU-MIMO signal detection lies in the use of deep learning technique. The basic idea is to model the entire MU-MIMO system as a DNN, then end-to-end optimization can be implemented by using deep learning algorithms. A relatively comprehensive state-of-the-art review can be found in [5]. Notably, a joint modulation and decoding optimization algorithm is proposed in [6], where the residual multilayer perceptron (ResMLP) is employed for modulation constellation design. In [7], an autoencoder-based structure is proposed to generate noncoherent space-time codes. In [8], compressed sensing (CS) based algorithm is proposed to tackle the noncoherent detection problem particularly in massive machine-type communications (mMTC). Apart from the existing literature, our preliminary work in [9] provides an end-to-end optimization solution for the MU-MIMO systems.

Despite their advantages, current deep learning-based joint transmitter and noncoherent receiver optimization approaches are still challenged by the signal processing scalability with respect to the size of MU-MIMO networks. It has been shown that most of the existing algorithms can only perform well when the size of the MU-MIMO system is relatively small (e.g. 2×4 or even smaller). When the spatial-domain user load increases, their detection performance decreased rapidly due to the increasing inter-user interference (IUI).

Motivated by this observation, we fundamentally rethink the design of deep learning-based MU-MIMO transmitter and noncoherent receiver. By exploiting the time-domain degree of freedom (DoF), more robust solutions have been proposed towards this problem. Main contributions of this paper include:

- Two groups of deep learning based joint transmitter and noncoherent receiver optimization approaches for MU-MIMO systems. One group is called pilot-aided waveform, which is motivated by the traditional pilot-based waveform design. The key novelty of this approach mainly lies in the receiver side, since the received pilot symbols are utilized for DNN-based sequence-level signal detection rather than channel estimation. The other group is called learning-based waveform, where the multiuser waveform is partially or even completely designed by using neural networks. And the novelty of this approach is mainly focused on the multiuser waveform design at the transmitter side. It is shown that the pilot-aided waveform design outperforms the conventional least

squares (LS) channel estimation solution on small-size MU-MIMO systems. Meanwhile, the learning-based waveform design largely improves the traditional channel estimation based solutions in various communication scenarios. Beside, all proposed approaches bypass channel inversion or factorization which are needed for most of the noncoherent detection approaches. Therefore, the required computational complexities are much lower.

- The development of a novel weight initialization method for the proposed learning-based waveform design, termed symmetrical-interval initialization. It is found that the traditional weight initialization method can result in a training imbalance among different users. To tackle this issue, the proposed approach restricts the intervals for weight initialization and yields a much better convergence performance in deep neural network (DNN) training phase.

II. SYSTEM MODEL AND PROBLEM STATEMENT

A. MU-MIMO Uplink Model

Consider MU-MIMO uplink communications, where M user terminals (UTs) simultaneously communicate to an uplink access point (AP) with N receive antennas ($N \geq M$). The MU-MIMO channel is assumed to be block-fading, i.e., the channel remains unchanged within the coherence time T , and each UT employs a single transmit-antenna¹ to send a temporal sequence. For each transmission block of duration T , the received signal block is represented by

$$\mathbf{Y} = \mathbf{X}\mathbf{H} + \mathbf{V} \quad (1)$$

where $\mathbf{Y} \in \mathbb{C}^{T \times N}$ stands for the received signal block over T time slots, $\mathbf{X} \in \mathbb{C}^{T \times M}$ for the transmitted signal block, $\mathbf{H} \in \mathbb{C}^{M \times N}$ for the MU-MIMO channel matrix, and $\mathbf{V} \in \mathbb{C}^{T \times N}$ for the additive white Gaussian noise (AWGN) with each element independently drawn from $CN(0, \sigma^2 \mathbf{I})$. Moreover, \mathbf{I} is the identity matrix. Let $\mathbf{x}_m \in \mathbb{C}^{T \times 1}$ be the m^{th} column of \mathbf{X} . The average transmission power of each UT is regularized by

$$\frac{1}{T} \mathbb{E} [\mathbf{x}_m^H \mathbf{x}_m] \leq \delta_m P, \quad m \in \{1, 2, \dots, M\} \quad (2)$$

subject to $\delta_m \geq 0$ and $\sum_{m=1}^M \delta_m = 1$, where P is the total power budget, $\mathbb{E}(\cdot)$ is the expectation, and $[\cdot]^H$ is the matrix Hermitian.

B. Ambiguities in Noncoherent Detection

Suppose: A1) the channel matrix \mathbf{H} is unknown at the receiver side, and A2) elements in \mathbf{x}_m can be mutually correlated. The receiver aims to reconstruct the transmitted signal block \mathbf{X} from \mathbf{Y} through noncoherent sequence detection. The maximum a posteriori (MAP) estimates of \mathbf{X} is given by

$$\hat{\mathbf{X}} = \arg \max_{\mathbf{X}} p_{\mathbf{X}|\mathbf{Y}}(\mathbf{X}|\mathbf{Y}) \quad (3)$$

¹We assume each user having a single antenna to focus our presentation on the key ideas. An extension to multiple antennas is trivial.

subject to \mathbf{X} drawn from a finite-alphabet set $\mathcal{A} = \{\Theta_1, \dots, \Theta_J\}$, where $\Theta_j \in \mathbb{C}^{T \times M}$ and J the size of \mathcal{A} . The m^{th} column of Θ_j is the m^{th} UT's codeword, denoted by \mathbf{c}_m , which is independently drawn from their specific codebooks \mathbf{C}_m . Assuming each UT's codebook having L codewords, then we have $J = L^M$.

Theoretically, there are two factors that might cause a detection error in (3). One is the white Gaussian noise \mathbf{V} , and the other is the MU-MIMO channel \mathbf{H} (i.e. channel ambiguity). The noise effect has been well studied in [10], our focus is mainly on the channel ambiguity which should be well addressed in the proposed approaches.

Definition 1 (Channel Ambiguity): It is called channel ambiguity that the transmitted signal block \mathbf{X} is not uniquely determined by the received signal block \mathbf{Y} even in the noiseless case. This is one of the dominating factors that limits the application of noncoherent signal detection in MU-MIMO systems.

A natural solution towards this problem is to send a pilot sequence to estimate the fading coefficients [11], and then use the estimated channel to communicate. Although the channel estimation solution is outside the scope of noncoherent detection, it is closely related to the proposed pilot-aided waveform approach due to the same waveform format. Therefore, we provide a brief analysis to improve the readability of this paper.

Consider the short coherence time case, where the coherent interval $T < K + N$ with $K = \min\{M, N\}$. The training phase lasts T_τ time samples and the time duration for data transmission equals to $T_d = T - T_\tau$. In order to estimate the N -by- M channel coefficients, we will need at least $(N) \times (M)$ measurements at the receiver [12]. Therefore, the optimum length of the training interval is $T_\tau = M$ and the total DoF for communication is at most

$$D_{\text{pilot}} = M(1 - \frac{M}{T}) \quad (4)$$

and the result capacity lower bound with optimum power allocation at high signal-to-noise ratios (SNR) is given by

$$C_{\text{pilot}} \geq (1 - \frac{M}{T}) \mathbb{E} \left[\log \det \left(\mathbf{I}_M + \frac{1}{\left(\sqrt{1 - \frac{M}{T}} + \sqrt{\frac{M}{T}} \right)^2} \cdot \frac{\hat{\mathbf{H}} \hat{\mathbf{H}}^H}{M} \cdot \rho \right) \right] \quad (5)$$

where ρ is the expected received SNR at each receive antenna, and $\hat{\mathbf{H}}$ the normalized channel estimate [11]. Intuitively, the training based algorithm suffers a fractional DoF gap of $(M)/(T)$ from the ideal DoF. In Section III, we will demonstrate that the proposed learning-based approaches have the ability to mitigate the DoF loss.

III. DEEP LEARNING BASED JOINT TRANSMITTER AND NONCOHERENT RECEIVER DESIGN

A. Pilot-aided Waveform Design

Definition 2: It is called pilot-aided waveform design when the multiuser waveform is formed by the traditional MU-MIMO pilot symbols and the information-bearing symbols; as shown in Fig. 1.

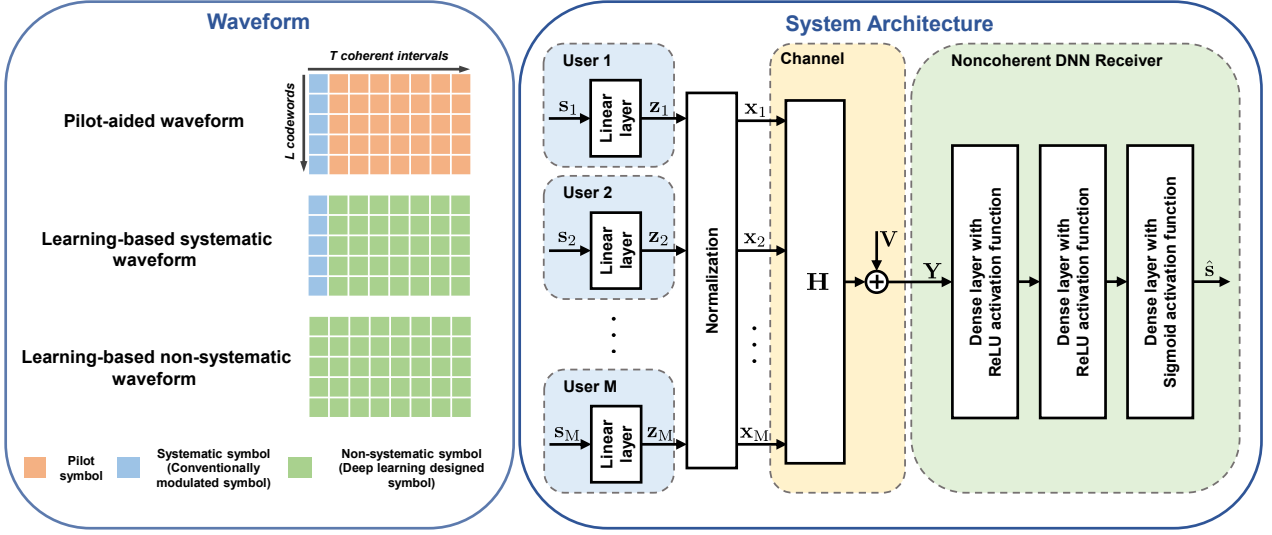


Fig. 1. The proposed system architecture and waveforms for MU-MIMO joint transmitter and noncoherent receiver optimization.

We start from the introduction of the basic signal model, the two-part training and data process is equivalent to partitioning the matrix in (1) as

$$\mathbf{X} = \begin{pmatrix} \mathbf{X}_\tau \\ \mathbf{X}_d \end{pmatrix}, \quad \mathbf{Y} = \begin{pmatrix} \mathbf{Y}_\tau \\ \mathbf{Y}_d \end{pmatrix} \quad (6)$$

where \mathbf{X}_τ and \mathbf{X}_d stand for the matrices of training and data samples, respectively; and \mathbf{Y}_τ and \mathbf{Y}_d for the corresponding received signal blocks. As aforementioned, \mathbf{X}_d might not be uniquely determined by \mathbf{Y}_d due to channel ambiguity. Later, we will introduce how training matrices \mathbf{X}_τ and \mathbf{Y}_τ can be used to mitigate the uncertainty.

For pilot-aided waveform design, the transmitter side does not contain any neural networks. The linear layers are a group of predefined codebooks $\mathbf{W}_m^{(p)} \in \mathbb{C}^{L \times T}$, $1 \leq m \leq M$, with each consist of both pilot component and data component as described in (6). The input to the linear layer is a one-hot vector, denoted by \mathbf{s}_m , $1 \leq m \leq M$, with the size of $(L) \times (1)$, and \mathbf{s}_m follows the uniform distribution. The output is $\mathbf{z}_m = \mathbf{W}_m^{(p)T} \mathbf{s}_m$, $1 \leq m \leq M$, which is one of the codeword in the predefined codebook. Intuitively, \mathbf{s}_m serves as a waveform selector. By combining the codewords from all M users, we are able to form the signal block \mathbf{X} . At the receiver side, DNN plays a central role for multiuser noncoherent signal detection. The input to the DNN receiver is obtained by reshaping the signal matrix \mathbf{Y} into a column vector \mathbf{y} . It is worth noting that the communication signals are normally modeled as complex-valued symbols, but most of the deep learning algorithms are based on real-valued operations. To facilitate the learning and communication procedure, it is usual practice to convert complex signals to their real signal equivalent version by concatenating their real and imaginary parts² (see [13]–[19]) which can be described as

$$\mathbf{y}_{\text{real}} = \begin{bmatrix} \Re(\mathbf{y}) \\ \Im(\mathbf{y}) \end{bmatrix} \quad (7)$$

²For the sake of mathematical notation simplicity, we will not use doubled size for the rest of this paper.

The noncoherent DNN receiver consists of three layers: two dense layers with ReLU activation function followed by a dense layer with Sigmoid activation function. The output of the DNN receiver $\hat{\mathbf{s}}$ is an estimate of the original information-bearing bits. Such an estimate can be trained by using supervised learning algorithms with the objective of minimizing the difference between the network estimate $\hat{\mathbf{s}}$ and the ground-truth training label \mathbf{s} , where the latter can be obtained by using the codebook combination approaches (see [19, Section II-B&C] for more detailed descriptions).

Proposition 1: Given the received signal \mathbf{Y} and the supervisory training target \mathbf{s} , deep learning will establish the link between \mathbf{Y} and \mathbf{X}_d according to the MAP probability $p(\mathbf{s}|\mathbf{Y}) = p(\mathbf{X}_d|\mathbf{Y})$.

For a fixed channel matrix \mathbf{H} , we can easily obtain the estimate of \mathbf{X}_d according to the MAP probability $p(\mathbf{X}_d|\mathbf{Y}_d)$ even without the pilot component. Problem becomes difficult when \mathbf{H} is randomly varying. In this case, \mathbf{Y}_τ can be employed to mitigate the channel uncertainty in noncoherent signal detection. From mutual information point of view we have

$$\begin{aligned} I(\mathbf{Y}_\tau, \mathbf{Y}_d; \mathbf{X}_d) &= I(\mathbf{Y}_d; \mathbf{X}_d | \mathbf{Y}_\tau) + I(\mathbf{Y}_\tau; \mathbf{X}_d) \\ &= I(\mathbf{Y}_d; \mathbf{X}_d | \mathbf{Y}_\tau) \\ &\approx I(\mathbf{Y}_d; \mathbf{X}_d | \mathbf{H}) \\ &\geq I(\mathbf{Y}_d; \mathbf{X}_d) \end{aligned} \quad (8)$$

where $I(\mathbf{Y}_\tau; \mathbf{X}_d) = 0$ because \mathbf{X}_d is independent of \mathbf{Y}_τ , and the equality holds if and only if \mathbf{H} is fixed. Intuitively, the pilot signal block is able to mitigate the channel uncertainty to a certain level. Generally, one of the major advantages of the pilot-aided waveform design is that it bypasses channel matrix inversion or factorization which are needed in most of the channel estimation solutions. Therefore, the required computational complexity is much lower than the others. Despite, such an approach still suffers a fractional DoF loss which will directly affect the system capacity as we previously shown in (5).

B. Learning-based Waveform Design

Definition 3: It is called learning-based waveform design when the multiuser waveform is partially or even completely designed by neural network. If the information-bearing symbol is directly embedded in the designed waveform, it is called systematic waveform. Otherwise, it is called non-systematic waveform, where no artificial design is involved; as shown in Fig. 1.

For learning-based waveform design, the transmitter side is modeled as a group of linear layers, with each weighting matrix can be viewed as a user-specific codebook. The difference between systematic and non-systemic waveform is the number of learnable parameters (i.e. non-systematic symbols) inside the weighting matrix. These parameters will be optimized by the model during the training procedure. In systematic waveform, the total number of learnable parameters is $(L) \times (T-1)$, together with the $(L) \times (1)$ systematic part, forms the weighting matrix $\mathbf{W}_m^{(s)}$, $1 \leq m \leq M$. On the other hand, the total number of learnable parameters for non-systematic waveform is $(L) \times (T)$ since it does not contain any artificial design. The input to the linear layer is again a one-hot vector \mathbf{s}_m , $1 \leq m \leq M$, with the size of $(L) \times (1)$. And the output of the linear layer is again one of its column elements. By normalizing the signal power, the designed signal can be transmitted through wireless channel. Besides, the DNN-based noncoherent receiver remains unchanged as we have introduced in the previous section.

Proposition 2 (see [9]): The goal of multiuser joint waveform design is to find a set $\mathcal{A} = \{\Theta_1, \dots, \Theta_J\}$ (or equivalently \mathbf{C}_m , $\forall m$) that minimizes the error probability.

Given the waveform set to be equally probable, the probability of signal Θ_i being detected incorrectly in the noise-free case can be expressed as

$$\mathcal{P}_\epsilon = \mathbb{E} \left(\frac{\sum_{i \neq j} p(\Theta_j^{-1} \Theta_i \mathbf{H}_i)}{\sum_{j=1}^J p(\Theta_j^{-1} \Theta_i \mathbf{H}_i)} \right) \quad (9)$$

where $\mathbf{H}_i \triangleq \Theta_i^{-1} \mathbf{Y}$ in the noiseless case. Thus, the codebook design aims to minimize the following objective function

$$\min_{\mathcal{A}} \mathcal{P}_\epsilon = \min_{\mathcal{A}} (1 - \Gamma(\mathbf{H}_i, \Theta_i)) \quad (10)$$

where

$$\Gamma(\mathbf{H}_i, \Theta_i) \triangleq \mathbb{E} \left(\frac{p(\mathbf{H}_i)}{\sum_{j=1}^J p(\Theta_j^{-1} \Theta_i \mathbf{H}_i)} \right) \quad (11)$$

In general, this optimization problem is mathematically intractable and highly depends on the probability distribution of \mathbf{H}_i . We might employ Cauchy-Schwarz inequality to obtain

$$\Gamma(\mathbf{H}_i, \Theta_i) \leq \sqrt{\mathbb{E} \left(\frac{p(\mathbf{H}_i)}{(\sum_{j=1}^J p(\Theta_j^{-1} \Theta_i \mathbf{H}_i))^2} \right) \mathbb{E}(p(\mathbf{H}_i))} \quad (12)$$

and the upper bound can be achieved at

$$p(\mathbf{H}_i) + \sum_{i \neq j} p(\Theta_j^{-1} \Theta_i \mathbf{H}_i) = \lambda \quad (13)$$

where λ is a constant number. Generally, it is mathematically challenged to obtain sufficient conditions for (10) and the optimization problem in (13) is an integer linear programming (ILP) problem which is NP hard. The above motivates us to utilize deep learning technique to find an acceptable waveform set \mathcal{A} . Moreover, since the proposed deep learning algorithms do not have pilot-overhead, it is trivial to justify that the achievable DoF for communication is M without any fractional loss.

C. Complexity Analysis

The computational complexity required for training the pilot-aided waveform design approach is $\mathcal{O}(|\mathcal{B}|N^2)$ per iteration, where $|\mathcal{B}|$ is the size of mini-batch; and $\mathcal{O}(N^2)$ per detection after training finished. The complexity is dominated by the matrix multiplication since the proposed network architecture only involves a feedforward neural network with several layers. The learning-based waveform design has the same complexity of $\mathcal{O}(N^2)$ since it has similar architecture with the pilot-aided waveform design. To put this in perspective, the LS channel estimation with zero forcing (ZF) equalization has a complexity of $\mathcal{O}(N^3)$ as matrix inversion is needed, but it is non-iterative and no training is required. Besides, the LS channel estimation with maximum-likelihood sequence detection (MLSD) has a complexity of $\mathcal{O}(L^M)$.

IV. SIMULATION RESULTS AND EVALUATION

A. Implementation Details

For pilot-aided waveform design, the training data consists of a number of randomly generated pairs $\mathbf{p}^{(i)} = \{\mathbf{s}^{(i)}, \mathbf{y}^{(i)}\}$, where $\mathbf{y}^{(i)}$ is obtained by transmitting pilot-aided signal blocks $\mathbf{X}^{(i)}$ through a random Rayleigh block-fading channel $\mathbf{H}^{(i)}$, and $\mathbf{s}^{(i)}$ is the referenced training target as we introduced in Section III-A. For learning-based waveform design, the training input is a group of one-hot vectors $\mathbf{s}_m^{(i)}$, $1 \leq m \leq M$, and the supervisory training output is again $\mathbf{s}^{(i)}$ by using codebook combination approaches [19].

The neural network is trained by using stochastic gradient descent (SGD) algorithm with Adam optimizer at early training stage. After a certain number of training epochs, we removes the Adam optimizer and only SGD algorithm is used to train the network until converging since SGD is believed to offer better convergence performance during final training phase [20]. The learning rate is set to be 0.001 and the size of mini-batch is 200. The loss function is categorical cross entropy which is defined as

$$\mathcal{L}(\mathbf{s}^{(i)}, \hat{\mathbf{s}}^{(i)}) = -\frac{1}{|\mathcal{B}|} \sum_{\mathbf{p}^{(i)} \in \mathcal{B}} \mathbf{s}^{(i)} \log \hat{\mathbf{s}}^{(i)} \quad (14)$$

where \mathcal{B} is the training set of a mini-batch.

In addition to these basic settings, here we also propose a novel weight initialization method for the learning-based waveform design. It is well known that weight initialization plays an important role in contributing to the DNN convergence performance. The traditional method,

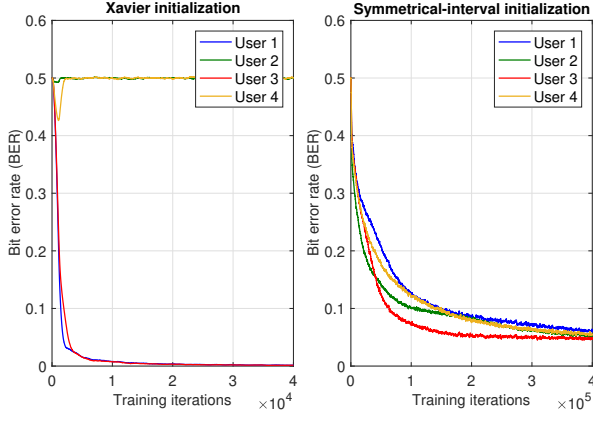


Fig. 2. The convergence performance of the Xavier initialization (left) and the proposed symmetrical-interval initialization method (right).

TABLE I
LAYOUT OF THE ARTIFICIAL NEURAL NETWORK (ANN)

Layer	Output dimension
Input	$2NT$
Dense + ReLU	1024
Dense + ReLU	512
Dense + Sigmoid	$M \log L$

such as Xavier [21], is to generate weights by using the following heuristic

$$\mathbf{W} \sim U\left(0, \frac{1}{\sqrt{n}}\right) \quad (15)$$

where $U(a, b)$ denotes the uniform distribution in the interval $(a - b, a + b)$ and n is the size of the input. However, such a method could result in a user imbalance problem. In Fig. 2 (left), we found that two users fails to converge as their detection error rate remains unchanged at 0.5. This is because the initialized weighting matrix \mathbf{W}_m , $1 \leq m \leq M$ might have its column elements differ by orders of magnitude before entering the normalization function. Therefore, individual user's waveform dominates the entire transmitted signal in training phase. To tackle this issue, we proposed a novel weight initialization method, termed symmetrical-interval initialization which randomly generates the weighting matrix elements within a pair of symmetrical intervals as described in the following equation

$$\mathbf{W} \sim U\left(\left(-\frac{1}{\sqrt{n}}, \zeta\right) \cup \left(\frac{1}{\sqrt{n}}, \zeta\right)\right) \quad (16)$$

where ζ is an arbitrary constant one order of magnitude smaller than $1/\sqrt{n}$. By such means, the convergence performance of the proposed learning-based waveform design has been greatly improved as shown in Fig. 2 (right).

All simulations are run on a Dell PowerEdge R730 2x 8-Core E5-2667v4 server, and implemented in Matlab.

B. Simulation and Performance Evaluation

Our computer simulations are structured into two parts with respect to the size of MU-MIMO network. For pilot-

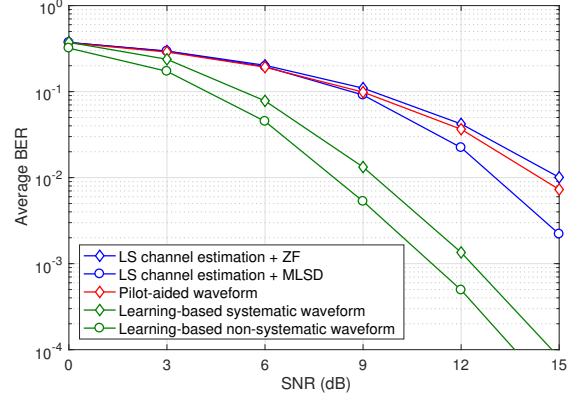


Fig. 3. Performance comparison among various schemes with $M = 4$, $N = 8$, $T_\tau = 4$, $T_d = 1$.

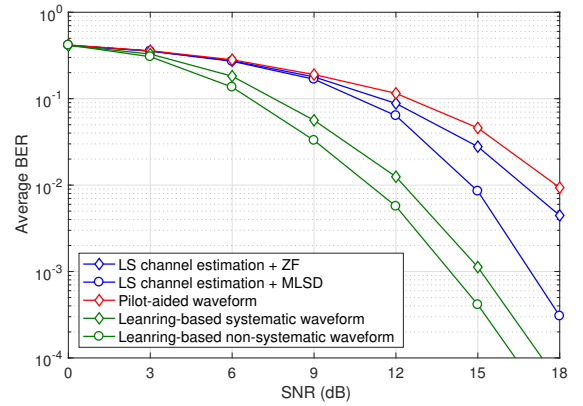


Fig. 4. Performance comparison among various schemes with $M = 8$, $N = 16$, $T_\tau = 8$, $T_d = 1$.

aided waveform design, the number of pilot symbols sent by each user is equal to the user number M in the simulation (i.e. $T_\tau = M$). For learning-based waveform design, the coherent interval T is set to be the same as the previous case to ensure the fair performance comparison. The modulation scheme is set to be the quadrature phase-shift keying (QPSK). The key metric utilized for performance evaluation is the average bit error rate (BER) over sufficient Monte-Carlo trails of block Rayleigh fading channels. The SNR is defined as the average received information bit-energy to noise ratio per receive antenna for the entire T coherent intervals. Besides, the neural network layout is listed in Table I.

Fig. 3 shows the average BER performance of the proposed deep learning approaches in 4-by-8 MU-MIMO system. The baselines for performance comparison are obtained by using the conventional LS channel estimation with ZF equalization or MLSD. The coherent time slot T is set to be 5. It is shown that the proposed pilot-aided waveform design slightly outperforms the conventional LS channel estimation with ZF equalization. The performance improvement is around 0.6 dB at BER of 10^{-2} . But the gap to the LS-MLSD solution is still around 1.5 dB at BER of 10^{-2} . Meanwhile, two learning-based waveform design approaches demonstrate their tremendous advan-

tages towards the conventional pilot-based algorithms. The BER improves about 3.7 dB for systematic waveform and 5 dB for non-systematic waveform at BER of 10^{-3} , respectively. This is reasonable since the time-domain redundancy obtained by removing the pilot symbols has been well exploited. Moreover, the non-systematic approach outperforms the systematic approach for approximately 1 dB at BER of 10^{-3} since the former provides higher flexibility for joint multiuser codebook design.

Fig. 4 shows the average BER performance of the proposed deep learning approaches in 8-by-16 MU-MIMO system. The baselines for performance comparison remain unchanged. The coherent time slot T is set to be 9. Different from the previous case, here the performance of the pilot-aided waveform slightly decreases with a BER gap around 1.3 dB compares with the conventional LS-ZF solution. This is due to the increasing IUI, which makes sequence-level signal detection more difficult. Meanwhile, the proposed learning-based approaches maintain a good performance which demonstrates their scalability with respect to the size of the MU-MIMO network. The BER gap between systematic waveform and non-systematic waveform to the conventional LS-MLSD solution is approximately 3 dB and 2 dB at BER of 10^{-3} , respectively.

V. CONCLUSION

This paper aims to handle the joint transmitter and noncoherent receiver design for MU-MIMO systems. It has been shown that DNN receiver can realize noncoherent signal detection directly under the conventional pilot-based signal model. Without the requirement of channel inversion, it can outperform the LS channel estimation with ZF equalization in small-size MU-MIMO systems. The performance can be further improved by adopting the learning-based waveform design, where the transmitted waveforms are jointly optimized by deep learning algorithms. By such means, the detection performance can be further improved for more than 5 dB at high SNR range in various communication scenarios.

ACKNOWLEDGEMENT

The work was supported in part by European Commission under the framework of the Horizon2020 5G-Drive project, and in part by 5G Innovation Centre (5GIC) HEFEC grant.

REFERENCES

- [1] S. Yang and L. Hanzo, "Fifty years of MIMO detection: The road to large-scale MIMOs," *IEEE Commun. Surv. Tut.*, vol. 17, no. 4, pp. 1941–1988, Fourthquarter 2015.
- [2] M. A. Albreem, M. Juntti, and S. Shahabuddin, "Massive MIMO detection techniques: A survey," *IEEE Commun. Surv. Tut.*, vol. 21, no. 4, pp. 3109–3132, Fourthquarter 2019.
- [3] A. Schenk and R. F. H. Fischer, "Noncoherent detection in massive MIMO systems," in *WSA 2013; 17th Int. ITG Workshop on Smart Antennas*, March 2013, pp. 1–8.
- [4] F. Alsifiany, A. Ikhlef, and J. A. Chambers, "On differential modulation in downlink multiuser MIMO systems," *CoRR*, vol. abs/1707.01603, 2017. [Online]. Available: <http://arxiv.org/abs/1707.01603>
- [5] C. Zhang, P. Patras, and H. Haddadi, "Deep learning in mobile and wireless networking: A survey," *IEEE Commun. Surv. Tut.*, vol. 21, no. 3, pp. 2224–2287, thirdquarter 2019.
- [6] Y. Wang and T. Koike-Akino, "Learning to modulate for non-coherent MIMO," *arXiv e-prints*, p. arXiv:1903.03711, Mar. 2019.
- [7] M. A. ElMossallamy, Z. Han, M. Pan, R. Jantti, K. G. Seddik, and G. Y. Li, "Noncoherent MIMO codes construction using autoencoders," in *2019 IEEE Global Commun. Conf. (GLOBECOM)*, Dec 2019, pp. 1–6.
- [8] K. Senel and E. G. Larsson, "Joint user activity and non-coherent data detection in mMTC-enabled massive MIMO using machine learning algorithms," in *WSA 2018; 22nd Int. ITG Workshop on Smart Antennas*, March 2018, pp. 1–6.
- [9] S. Xue, Y. Ma, N. Yi, and R. Tafazolli, "Unsupervised deep learning for MU-SIMO joint transmitter and noncoherent receiver design," *IEEE Wire. Commun. Lett.*, vol. 8, no. 1, pp. 177–180, Feb 2019.
- [10] T. O'Shea and J. Hoydis, "An introduction to deep learning for the physical layer," *IEEE Trans. on Cogn. Commun. and Netw.*, vol. 3, no. 4, pp. 563–575, 2017.
- [11] B. Hassibi and B. M. Hochwald, "How much training is needed in multiple-antenna wireless links?" *IEEE Trans. on Inf. Theory*, vol. 49, no. 4, pp. 951–963, 2003.
- [12] Lizhong Zheng and D. N. C. Tse, "Communication on the grassmann manifold: a geometric approach to the noncoherent multiple-antenna channel," *IEEE Trans. on Inf. Theory*, vol. 48, no. 2, pp. 359–383, 2002.
- [13] S. Xue, Y. Ma, A. Li, N. Yi, and R. Tafazolli, "On unsupervised deep learning solutions for coherent MU-SIMO detection in fading channels," in *ICC 2019 - 2019 IEEE Int. Conf. on Commun. (ICC)*, 2019, pp. 1–6.
- [14] S. Xue, Y. Ma, and R. Tafazolli, "An orthogonal-SGD based learning approach for MIMO detection under multiple channel models," *arXiv e-prints*, p. arXiv:2002.10847, Feb. 2020.
- [15] H. He, C. Wen, S. Jin, and G. Y. Li, "A model-driven deep learning network for MIMO detection," in *2018 IEEE Global Conf. on Signal and Inf. Processing (GlobalSIP)*, 2018, pp. 584–588.
- [16] N. Samuel, T. Diskin, and A. Wiesel, "Learning to detect," *IEEE Trans. on Signal Processing*, vol. 67, no. 10, pp. 2554–2564, 2019.
- [17] A. Li, Y. Ma, S. Xue, N. Yi, R. Tafazolli, and T. E. Hodgson, "Unsupervised deep learning for blind multiuser frequency synchronization in OFDMA uplink," in *ICC 2019 - 2019 IEEE Int. Conf. on Commun. (ICC)*, May 2019, pp. 1–6.
- [18] A. Li, Y. Ma, S. Xue, N. Yi, and R. Tafazolli, "A carrier-frequency-offset resilient OFDMA receiver designed through machine deep learning," in *2018 IEEE 29th Annu. Int. Symp. on Pers., Indoor and Mobile Radio Commun. (PIMRC)*, Sep. 2018, pp. 1–6.
- [19] S. Xue, Y. Ma, N. Yi, and T. E. Hodgson, "A modular neural network based deep learning approach for MIMO signal detection," *arXiv e-prints*, p. arXiv:2004.00404, Apr. 2020.
- [20] S. Bock, J. Goppold, and M. Weiß, "An improvement of the convergence proof of the ADAM-optimizer," *arXiv e-prints*, p. arXiv:1804.10587, Apr. 2018.
- [21] X. Glorot and Y. Bengio, "Understanding the difficulty of training deep feedforward neural networks," in *Proceedings of the Thirteenth International Conference on Artificial Intelligence and Statistics*, ser. Proceedings of Machine Learning Research, Y. W. Teh and M. Titterton, Eds., vol. 9. Chia Laguna Resort, Sardinia, Italy: PMLR, 13–15 May 2010, pp. 249–256.